ACS OMEGA

Open Access

http://pubs.acs.org/journal/acsodf

Article

Effects of Pressurized Pyrolysis on the Chemical and Porous Structure Evolution of Coal Core during Deep Underground Coal Gasification

Maofei Niu, Lin Xin,* Weimin Cheng, Shuqin Liu, Bowei Wang, and Weihao Xu

Cite This: *ACS Omega* 2023, 8, 40153−40161

Read Online

ACCESS | Metrics & More | Article Recommendations

ABSTRACT: During deep underground coal gasification, the semicoke produced by the pyrolysis of dense coal cores is an important material for its gasification and combustion. In this paper, pressurized pyrolysis experiments were carried out on dense coal cores at 700 °C and pressures of 1, 2, and 3 MPa using a shaft furnace. The resulting semicoke and raw coal were analyzed using the characterization methods such as the N_2 isothermal adsorption/desorption and scanning electron microscopy, Fourier transform infrared spectrometry (FTIR), and a pressurized thermogravimetric analyzer coupled with a FTIR spectrometer. The pyrolysis gas generation characteristics during pressurized pyrolysis were studied. The mechanisms of evolution of aliphatic functional groups and pore structures in semicoke during pressurized pyrolysis were revealed. The results indicate that the increase in pressure obviously changed the gas composition, most notably, the relative content of CH_4 and H_2 in the pyrolysis gas. The methane in the pyrolysis gas during pressurized pyrolysis of dense coal cores is mainly from the secondary reaction. As the pyrolysis pressure increased, the ratio of $-CH_2-/-CH_3$ became smaller, indicating that the pressure promoted the breakage of the long fat chains. With the increase of the pyrolysis pressure, the surface deformation of pressurized pyrolysis semicoke increases, and the pore structure becomes more abundant.

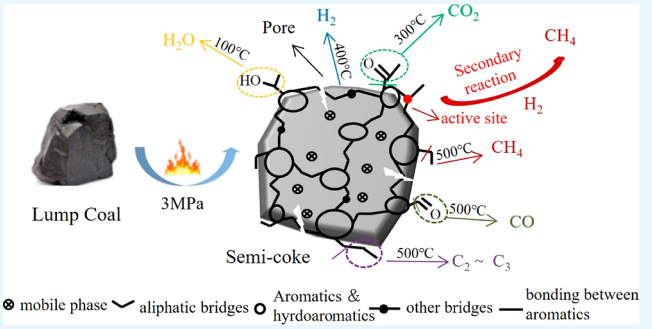

1. INTRODUCTION

In 2021, the total production and consumption of coal in China accounted for 67.0 and 56.0% of primary energy, respectively, which is mainly applied for electricity and heat generation or as syngas (for chemical synthesis).[1−3] Based on China's huge coal reserves, coal is expected to remain the dominant primary energy for a considerable period and will continue to contribute to China's socio-economic development for a long time to come.[4] The present global climate change has developed detailed emission reduction plans to tackle climate change. However, that range of plans still falls short of achieving the Paris Agreement's goal of emission reduction. For this reason, scholars have delved into the economic feasibility of carbon removal, such as biochar-based.[5] In September 2020, at the 75th United Nations General Assembly, the Chinese government made an important commitment to "peak carbon dioxide emissions by 2030 and carbon neutrality by 2060", which will guide China's national policy for medium- and long-term energy development.[6] Therefore, how to use coal resources efficiently, cleanly, and safely is an important part of China's "double carbon" goal and is also in line with China's energy strategy.[7,8]

Underground coal gasification (UCG) is the process of underground controlled combustion of coal in situ and a series of chemical reactions with gasification agents, converting the coal into a valuable gas product.[9,10] Coal gasification can also produce liquid fuels, such as methanol. Compared to fossil fuels, the combustion of methanol reduces nitrogen oxide, carbon dioxide emissions, and sulfur oxide emissions.[11] UCG technology has changed the traditional way of coal processing and its utilization. It has the advantages of coal mining and utilization with good safety performance, less investment and construction,[12,13] high economic efficiency,[14,15] and less environmental pollution.[16] Osman et al.[17] showed that captured CO_2 can be stored in geological formations, enabling large-scale carbon sequestration. Near-zero carbon emissions can be achieved using a combination of UCG carbon capture, utilization, and storage technology (CCUS). China's deep coal

Received: May 12, 2023
Accepted: October 2, 2023
Published: October 17, 2023

deposits are abundant, with proven depths of 1000−2000 m up to 2.7 trillion tons.[18] However, there are no technical and economic conditions for mining coal resources with a depth of 1000 m at present due to the influence of rock bursts.[19] Therefore, the UCG technology is extremely promising for deep coal mining. As an important supplementary technique for coal mining and utilization, UCG technology has, in recent years, been developed and advanced widely.[20,21] Pyrolysis gas is an important component of the UCG gas product. In addition, the semicoke produced by pyrolysis is the raw material for gasification and combustion. The pressure in the pyrolysis process is a very important factor.

In the process of UCG, when the oxygen in the UCG cavity is exhausted, heat accumulates in the coal seam, and strong pyrolysis reactions occur on both sides and in front of the coal wall. The structure of the coal char undergoes significant changes, such as expansion and deformation, during the devolatilization of coal. The structure of coal char is mainly dependent on changes in heating conditions such as temperature, heating rate, and pressure.[22] The effect of pressure on the pyrolysis process of coal is mainly manifested in two aspects, one is that the volatile fraction stays longer in the coal and its release is inhibited and the other is that the diffusion of the volatile fraction inside the coal particles increases, which obviously increases the secondary reaction.[23] Howaniec et al.[24] studied the properties of lignite coke produced at 1, 2, 3, and 4 MPa and 1273 K, and it revealed that the development of the porous structure of semicoke was enhanced with increasing pressure. Zhu et al.[25] showed that pressure affects the pyrolysis process mainly by influencing the secondary reaction of primary volatiles in coal particles. Xie et al.[26] showed that ion-exchanged alkali and alkaline earth metals in raw coal can promote the breakage of long aliphatic chains at pyrolysis pressures higher than 1 MPa. The physicochemical properties such as pore structure and microcrystalline structure of semicoke are an important basis for studying the gasification and combustion processes of coal char. However, the chemical structure evolution of dense coal cores under different pyrolysis pressures has rarely been reported.

In this article, pressurized pyrolysis experiments of coal cores were carried out through a pressurized pyrolysis device. The characterization methods such as Fourier transform infrared (FT-IR), X-ray diffraction (XRD), Brunauer−Emmett−Teller (BET), and pressurized thermogravimetric (TG)−FTIR were used to study the pyrolysis gas generation characteristics during pressurized pyrolysis. The mechanisms of evolution of aliphatic functional groups and pore structures in semicoke during pressurized pyrolysis were revealed. This paper provides a scientific basis for deep UCG to produce methane.

2. MATERIALS AND METHODS

2.1. Materials. The coal used in the experiments is long-flame coal located in Inner Mongolia, China, as shown in Figure 1. A sample of approximately 90 mm diameter raw coal was collected from the underground coal seam by means of drilling. The results of proximate analysis and ultimate analysis of raw coals have been described in our previous research.[27]

2.2. Experimental Method. A diagram of the experimental setup for pressurized pyrolysis of coal cores is depicted in Figure 2. The laboratory equipment mainly consists of four parts, including a high-pressure reactor (Φ 48.3 mm × 10.2 mm × 650.0 mm), a temperature control system, a liquid phase product condensation system, and a detection system.

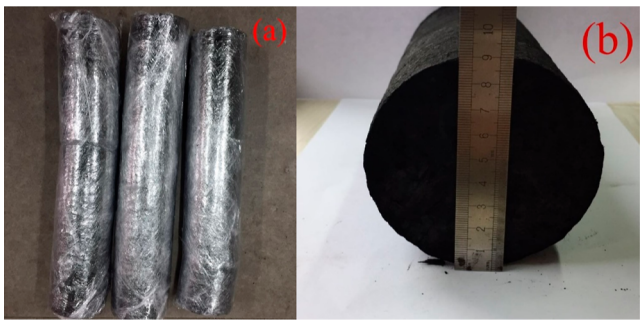

Figure 1. (a) Raw coal and (b) coal core (reprinted with permission from ref 27. copyright 2022 Elsevier).

Gas bags made of aluminum-plastic composite film are used to collect the gas produced by pressurized pyrolysis. The pyrolysis gas components were analyzed by gas chromatography (GC-2014C, Shimadzu, Japan).

First, the air in the experimental system is purged with a flow rate of 500 mL/min of nitrogen. After the high-pressure reactor leak test, the samples were heated at a rate of 10 °C/min to the target temperature and then held at that temperature for 30 min. The coal cores with a diameter of 24.5 mm and a mass of ca. 40 g were processed in a high-pressure reactor to produce semicokes under various pressure conditions of 0.1, 1, 2, and 3 MPa. The gas was collected during the experiment, and the semicoke was collected at the end. The gas produced by pyrolysis is mixed with pressurized nitrogen in the atmosphere for pressurized pyrolysis due to the outlet pressure control of the experimental unit.

2.3. Analysis and Characterization. The raw coal and semicoke samples were analyzed by a FT-IR spectrometer (Nicolet IS10, USA) in the spectral range of 4000−500 cm^{-1}. The samples were pressed by mixing semicoke samples with KBr powder at a mass ratio of 1:200 under a pressure of 1 MPa.

The nitrogen adsorption analysis was performed at 77 K using a Quantachrome instrument (NOVA100E, USA). The samples were outgassed under a vacuum at 120 °C for 12 h before exposure to the adsorbed gas. The specific surface area, mesopore area, and pore size distribution of the semicoke samples were tested separately. The pore size distribution was calculated using the Barrett−Joyner−Halenda (BJH) model based on the desorption isotherm.[28]

The microscopic morphology and pore structure of semicoke samples were characterized by scanning electron microscopy (SEM, SU8020, Japan) and energy-dispersive X-ray spectrometry (EDS, Japan).[29]

The pyrolysis of coal samples was carried out using a PTGA (Thermal Max 500, Thermal Cahn) coupled to FT-IR (NICOLET IS5, America). Approximately 10 mg samples were put into a pressurized TGA, and the system pressure and temperature were elevated to the selected values (0.1, 1.0, 2.0, and 3.0 MPa; 1000 °C). The TG experiment was carried out at a rate of 10 °C/min with a flow rate of 100 mL/min of argon as the carrier gas. The pyrolysis gas from the TG analyzer, with highly pure argon at a flow rate of 80 mL/min as the carrier gas, was fed into the online FT-IR spectrometer to detect its composition.

https://doi.org/10.1021/acsomega.3c03327
ACS Omega 2023, 8, 40153−40161

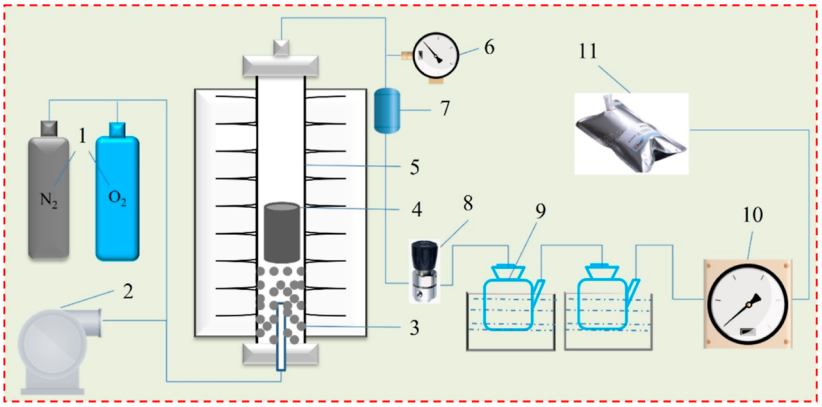

Figure 2. Diagram of the experimental setup for pressurized pyrolysis of coal cores: 1-nitrogen; 2-high-pressure pump; 3-Al_2O_3 porcelain ball; 4-raw coal; 5-reactor; 6-pressure gauge; 7-filter; 8-back-pressure value; 9-condenser; 10-wet flow; and 11-gas bags.

3. RESULTS AND DISCUSSION

3.1. Effects of Pyrolysis Temperature and Pressure on Syngas Composition. The effect of temperature on cumulative pyrolysis gas component content at 3 MPa is shown in Figure 3. When the pyrolysis temperature is less than

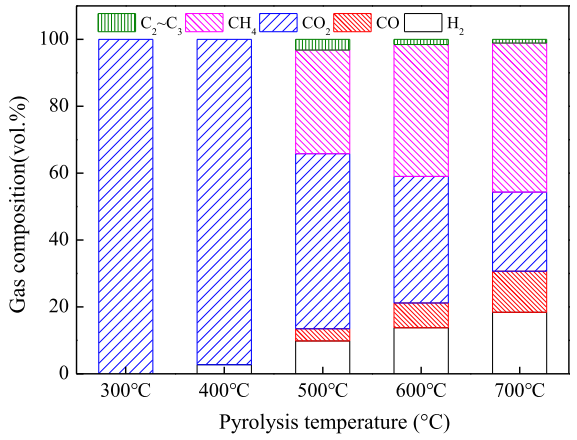

Figure 3. Effect of temperature on the cumulative pyrolysis gas component relative content at 3 MPa.

300 °C, it is the degasification and dehydration stage. The pyrolysis of coal starts at about 300 °C and is dominated by the decomposition of carboxyl groups in coal macromolecules, so the gas component is dominated by CO_2. When the pyrolysis temperature reached 400−500 °C, the chemical bond breakage in the macromolecular structure of coal began to be significantly enhanced, and the CH_4 and H_2 contents in the gas fraction increased significantly, which was consistent with the analytical results of FT-IR of semicoke. The carbonyl and ether bonds begin to break at temperatures of 400 and 700 °C to form CO, respectively. When the pyrolysis temperature is low, the gas component is mainly controlled by the pyrolysis temperature.

The effect of pressure on the cumulative pyrolysis gas component and the yield of gas at 700 °C are shown in Figure 4. The cumulative yield of pyrolysis gas increases with increasing pyrolysis pressure. Our previous studies have shown that pressure promotes the secondary cracking reaction of coal tar and produces small-molecule compounds. With the increase of pyrolysis pressure, the relative contents of CO_2 and CH_4 increased significantly, while the relative contents of CO

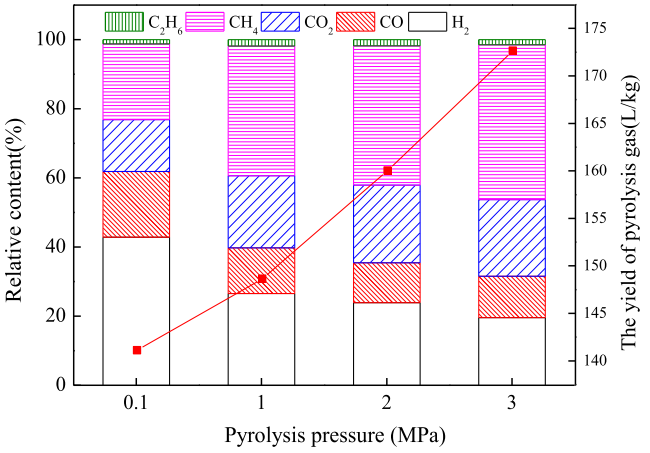

Figure 4. Effect of pressure on the cumulative pyrolysis gas component and the yield of gas at 700 °C.

and H_2 decreased, and the relative contents of $C_2 \sim C_3$ did not change significantly. When the pyrolysis pressure was increased from atmospheric pressure to 3 MPa, the relative content of H_2 in the pyrolysis gas decreased from 42.86 to 19.56%, while the relative content of CH_4 increased from 21.92 to 44.78%. The sum of the relative contents of CO_2 and CO is about 34% at different pyrolysis pressures. Therefore, the increase in pressure obviously changed the gas composition, most notably the relative content of CH_4 and H_2 in the pyrolysis gas.

It is shown that CH_4 is mainly derived from the cleavage of methoxy, alkyl side chains, and aryl methyl groups at low- and medium-temperature pyrolysis (<700 °C).[30,31] Most importantly, it was found that pyrolysis pressure greatly favored the formation of CH_4.[32] Our previous research shows that the pressure promoted the generation of CH_4 from the oxy-quaternary carbon chain as the active site in the aliphatic group. Combined with Section 3.1, it is concluded that the pressure promotes the secondary reaction, which in turn changes the components of the pyrolysis gas.

3.2. Online FTIR of Coal Sample Pyrolysis. During the process of atmospheric pressure pyrolysis of coal, coal tar and gases (CO_2, CO, H_2, CH_4, etc.) are mainly produced by primary pyrolysis.[33,34] In order to better understand the behavior of coal pyrolysis under pressure, gaseous products were analyzed by online infrared spectroscopy. The online infrared spectra for the pyrolytic gaseous products of coal are illustrated in Figure 5. Several volatile species including H_2,

https://doi.org/10.1021/acsomega.3c03327
ACS Omega 2023, 8, 40153−40161

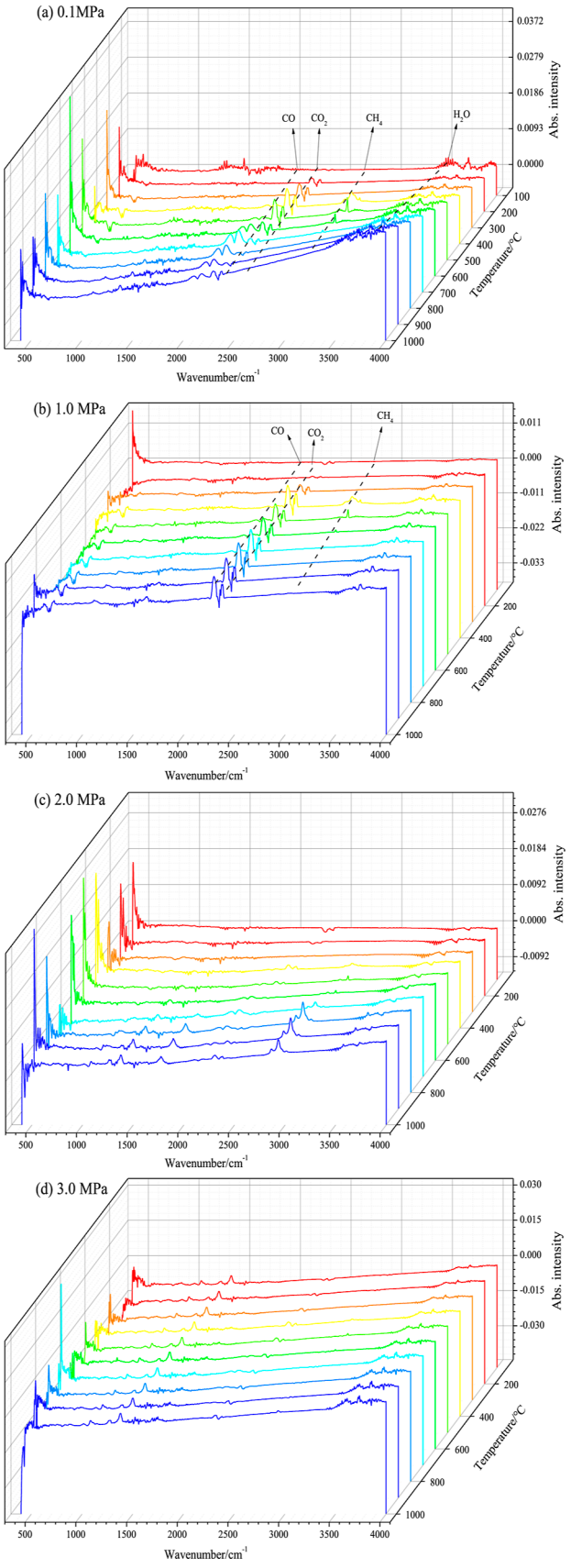

Figure 5. Online infrared spectra for the pyrolytic gaseous products of coal: (a) 0.1, (b) 1.0, (c) 2.0, and (d) 3.0 MPa.

CO_2, CO, CH_4, and H_2O were detected by FT-IR absorbance. At atmospheric pressure and 0.1 MPa, the absorption band of the infrared spectrum of CH_4 occurs between 400 and 700 °C. As the pyrolysis pressure increases, the intensity of the absorption bands representing the pyrolysis gases in the FT-IR spectrum gradually decreases. It is indicated that high external pressure hinders the release of moisture and volatiles from the primary pyrolysis process. Therefore, the gas component in the medium- and low-temperature pressurized pyrolysis process in dense coal cores is mainly controlled by secondary reactions.

In pressurized pyrolysis units, due to the secondary reactions of volatile fraction, chemical equilibrium between gas phase products and chemical reactions between gas components and semicoke result in large differences in the gas phase components. In contrast, pressurized TG−FTIR mainly investigates the mass loss of volatile fractions during the pyrolysis process. Therefore, there is a difference between the two results in the yield of the pyrolysis gas fraction.

3.3. Infrared Spectroscopy Analysis. *3.3.1. Evolution of the Chemical Structure of Semicoke during Pressurized Pyrolysis.* The FT-IR spectra of the semicoke under different temperatures of 3.0 MPa are shown in Figure 6. The

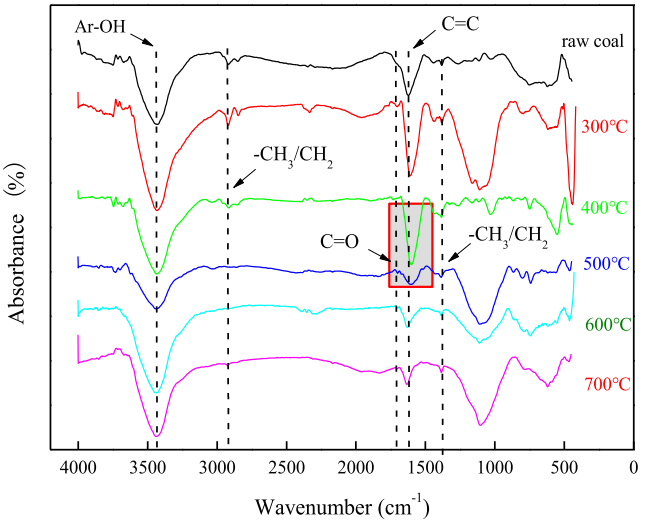

Figure 6. FT-IR spectra of the semicoke under different temperatures of 3.0 MPa.

absorption bands at 2999−2800 and 1520−1370 cm^{-1} are mainly caused by methyl($-CH_3$)/methylene($-CH_2-$) stretching vibration.[35] At the pressurized pyrolysis temperature of 400 °C, the absorption bands at the two locations weakened rapidly, and when the temperature was higher than 500 °C, the two absorption bands were close to disappearing. When the pressurized pyrolysis reached about 400 °C, the intensity of the absorption band of the C−C stretching vibration of the oxygen-substituted aromatics (1682−1520 cm^{-1}) began to weaken significantly. At 500 °C, the absorption band diminished to a minimum, indicating that the cleavage of carbonyl and carboxyl groups was completed at about 500 °C. To sum up, the intensity of the infrared absorption bands of various functional groups gradually weakened with the increase of the pyrolysis temperature, and the most significant weakening occurred at 400−500 °C, which was consistent with the generation temperature of gas components.

https://doi.org/10.1021/acsomega.3c03327
ACS Omega 2023, 8, 40153−40161

The FT-IR spectra of the semicoke under different pressures of 700 °C are shown in Figure 7. The absorption bands of

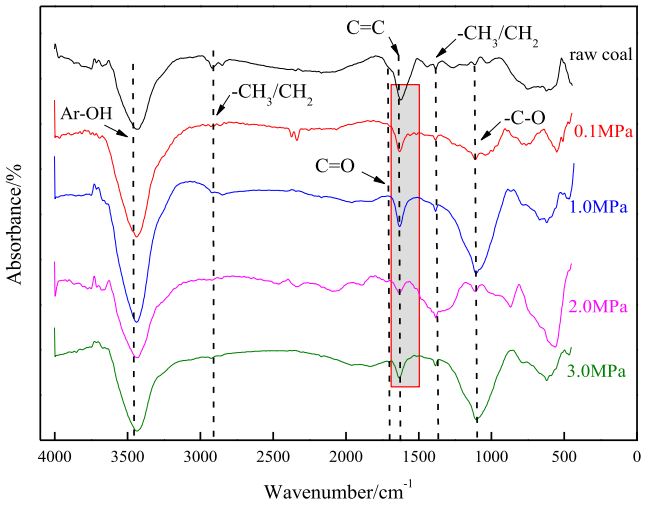

Figure 7. FT-IR spectra of coal coke under different pressures of 700 °C.

1682−1520 cm^{-1} are mainly caused by the C═C stretching vibration on the benzene ring. This absorption band decreases with the increase of the pyrolysis pressure, indicating that the process of pressurized pyrolysis is accompanied by the breakage of the aromatic ring, which is most significant at greater than 2 MPa. The absorption bands of methyl $-CH_3$ and methylene $-CH_2-$ (2999−2800 and 1520−1370 cm^{-1}) also weakened rapidly at a pyrolysis pressure of 2.0 MPa. The FT-IR spectra of the semicoke showed C−O bonds at 1000−1100 cm^{-1}, indicating the formation of C−O bonded compounds accompanying the pyrolysis process. To summarize, the intensity of the absorption band of the semicoke functional group gradually decreases with the increase of the pyrolysis pressure and decreases significantly after 2.0 MPa. Our previous study showed that the highest yield of gas was obtained at 3.0 MPa.[24]

3.3.2. Changes of the Aliphatic Structure in the 3000−2800 cm^{-1} Region at Elevated Pressures. The absorption bands of the FT-IR spectra of coal are divided into four main parts: hydroxyl groups (3600−3000 cm^{-1}), aliphatic structures (3000−2700 cm^{-1}), oxygen-containing functional groups (1800−1000 cm^{-1}), and aromatic structures (900−700 cm^{-1}). During the analysis of FT-IR of semicoke, the superposition of absorption bands of many functional groups occurs. Therefore, in order to determine the location and boundaries of the absorption bands of functional groups in coal coke, Origin 8.5 was used for peak fitting. Based on the results of the peak fitting of the FT-IR absorption bands, the characteristic parameters related to the structure and functional groups of the semicoke can be calculated. The temperature at

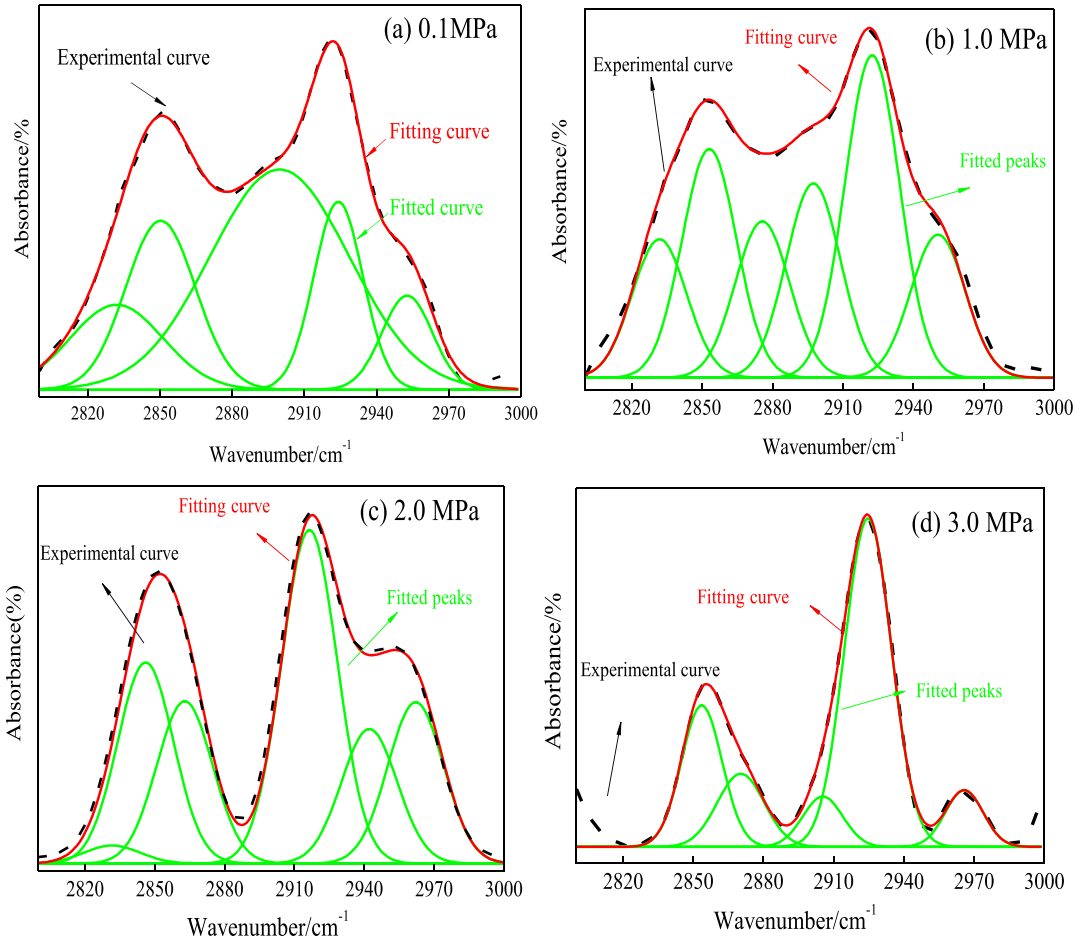

Figure 8. Fitting of aliphatic hydrocarbon (3000−2800 cm^{-1}) fractions in semicoke at different pyrolysis pressures of 700 °C (a) 0.1 MPa semicoke, (b) 1.0 MPa semicoke, (c) 2.0 MPa semicoke, and (d) 3.0 MPa semicoke.

https://doi.org/10.1021/acsomega.3c03327
ACS Omega 2023, 8, 40153−40161

Table 1. Relative Content of Aliphatic Hydrocarbons (3000−2800 cm^{-1}) in Semicoke at Different Pyrolysis Pressures

pressure/MPa	−CH−		$-CH_2-$		$-CH_3$		$-CH_2-/-CH_3$
	peak area	PCT/%	peak area	PCT/%	peak area	PCT/%	
0.1	0.0558	11.7568	0.1561	32.8806	0.2629	55.3625	1.6837
1.0	0.0949	16.4204	0.2692	46.5873	0.1463	25.3133	0.5433
2.0	0.0321	15.9512	0.1066	52.9079	0.0592	29.3611	0.5549
3.0	0.0066	6.9918	0.0695	73.6207	0.0183	19.3875	0.2633

which the chemical reactions of the functional groups in the macromolecular structure of coal occur varies with the cleavage of the aliphatic side chains occurring at lower temperatures. The changes in the aliphatic structure are highly correlated to the thermoelectricity of the coal. The results of the aliphatic structures (3000−2800 cm^{-1}) peak fitting of semicoke at different pyrolysis pressures are shown in Figure 8.

The results of the peak separation of aliphatic hydrocarbons (3000−2800 cm^{-1}) for the semicoke sample are shown in Table 1. The semicoke FT-IR spectra were located at 2870 and 2952, 2850 and 2925, and 2897 cm^{-1}, representing the absorption peaks of methyl ($-CH_3$), methylene ($-CH_2-$), and hypomethyl (−CH−) aliphatic hydrocarbons, respectively.[36] The ratio of $-CH_2-/-CH_3$ represents the chain length and the number of branched chains in aliphatic hydrocarbons, with larger values representing longer fatty chains and fewer branched chains.[37] As can be seen from Table 1, the ratio of $-CH_2-/-CH_3$ of the semicoke produced by atmospheric pressure pyrolysis is larger than that of the raw coal. It indicates that the macromolecular structure of coal undergoes the breakage of side chains, bridge bonds, etc., and more fatty chains are formed during atmospheric pressure pyrolysis. As the pyrolysis pressure increased, the ratio of $-CH_2-/-CH_3$ became smaller, indicating that the pressure promoted the breakage of the long fat chains.

3.4. Influence of Pressure on the Surface Properties of Semicokes. *3.4.1. Surface Morphology.* The pores in coal char are broadly classified into three types: micropores (<2.0 nm), mesopores (2.0−50 nm), and macropores (>50 nm).[38,39] The N_2 isotherms of semicoke at different pyrolysis pressures are shown in Figure 9. When the pyrolysis pressure is less than 2.0 MPa, the N_2 adsorption/desorption isothermal loop of semicoke is type I.[28] It indicates that there are abundant microporous structures in the semicoke produced by the pyrolysis of coal cores at different pressures. At a pyrolysis pressure of 3.0 MPa, the adsorption loop was converted to type II with mesopore adsorption properties. The adsorption amounts of the semicoke sample were the highest at 3.0 MPa, and its pore structure was the most developed. It shows that the semicoke produced by pressurized pyrolysis of coal cores has a complex porous structure and contains a certain amount of mesopores in addition to abundant micropores. This may be due to the increased pyrolysis pressure, which leads to the increased deformation of the semicoke and makes the pore structure in the semicoke develop more abundantly, consistent with the SEM results of the semicoke.

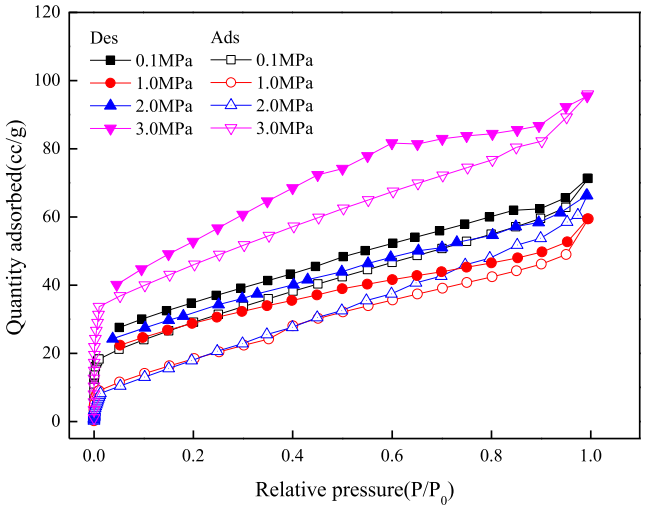

Figure 9. Nitrogen adsorption and desorption isotherms (77 K) for semicokes at different pyrolysis pressures of 700 °C.

The pore volume distribution of char at different pyrolysis pressures of 700 °C is shown in Figure 10. The value of the total pore volume of different pressurized pyrolysis semicokes is mainly determined by the mesopores. As the pyrolysis pressure increases, the value of the total pore volume of the semicoke decreases and then increases. When the pyrolysis pressure reached 3 MPa, the value of the total pore volume of semicoke increased significantly. It is shown that higher pressure can significantly improve the pore structure of coal coke, resulting in an increase in the total pore volume value.

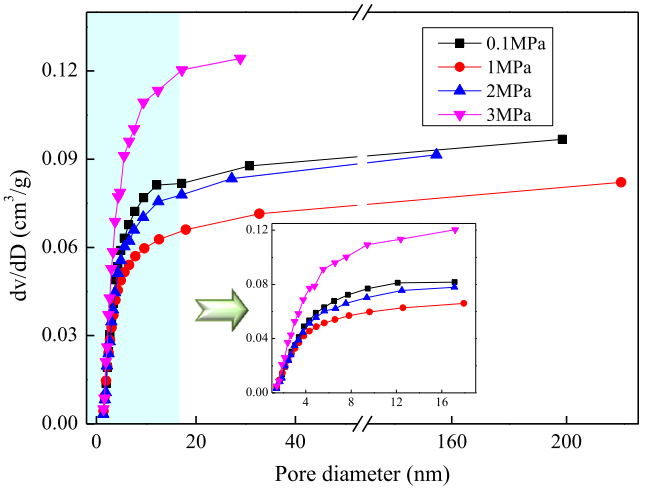

Figure 10. Pore volume distribution of char at different pyrolysis pressures of 700 °C.

The surface area and pore volume of semicoke with different pyrolysis pressures are shown in Figure 11. The surface area and pore volume of semicoke increase with increasing pyrolysis pressure. When the pyrolysis pressure was 3.0 MPa, the surface area and pore volume were the largest, and the development of a porous structure was the most significant. The swelling characteristics of coal affect the development of total pore volume and porosity.[40] It is indicated that the swelling characteristics of coal increase with increasing pyrolysis

https://doi.org/10.1021/acsomega.3c03327
ACS Omega 2023, 8, 40153−40161

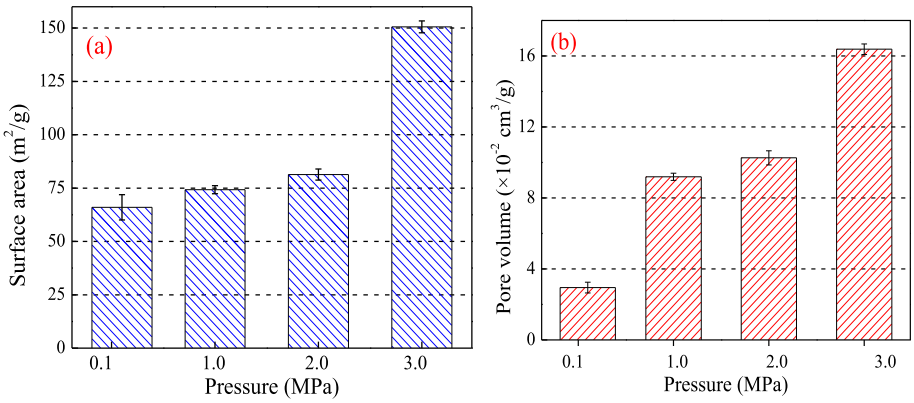

Figure 11. Effect of pyrolysis pressure on the (a) pore surface area and (b) coke pore volume of semicoke at 3 MPa.

pressure, which in turn affects the pore structure of the semicoke.[41]

The development of the pore structure of coal coke during pressurized pyrolysis is governed by the pressure and temperature. Besides, the moisture content, volatile content, and ash content of raw coal samples also affect the development of the coal coke pore structure. Among them, the evaporation of water in the raw coal during pyrolysis plays a leading role.[21] In addition, the degreasing of macromolecular structures during coal pyrolysis plays an important role in the growth of micropores.[42]

3.4.2. SEM Analysis of Semicoke. The microscopic morphology of semicoke samples at different pyrolysis pressures at 700 °C is presented in Figure 12. With the

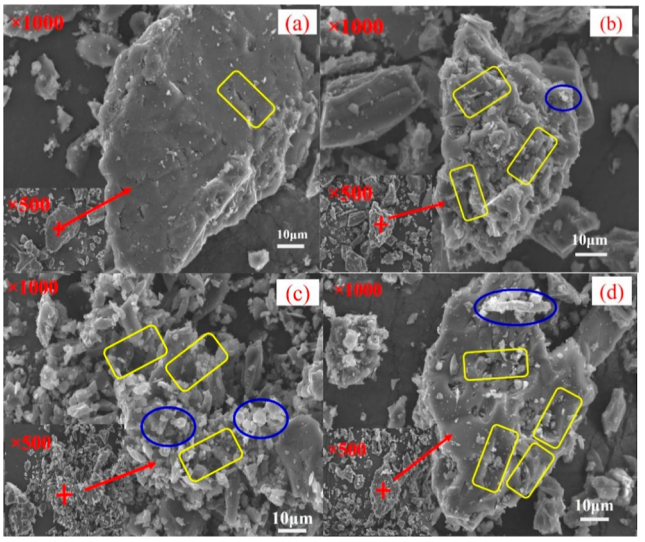

Figure 12. Microscopic morphology of semicoke at different pressures of 700 °C: (a) 0.1 MPa semicoke, (b) 1.0 MPa semicoke, (c) 2.0 MPa semicoke, and (d) 3.0 MPa semicoke.

increase of pyrolysis pressure, the pore structure of the semicoke surface becomes more abundant. The semicoke prepared under the atmosphere is dominated by a dense blocky structure. The pressurized pyrolysis semicoke has an obvious pore structure and more obvious deformation, with glass-like material attached to its surface. It can be clearly seen from Figure 12c,d that the microscopic morphology of the semicoke at 2.0 and 3.0 MPa is rougher with more fine particles attached, which may be caused by the melting deformation of the lower melting point vitreous material. At the same time, the pressure led to the generation of pore structures with a diameter of about 2 μm in the semicoke. Therefore, with the increase of pyrolysis pressure, the surface deformation of pressurized pyrolysis semicoke increases, and the pore structure becomes more abundant.

3.5. Pyrolysis Mechanisms for Gas Production from Coal Cores. The mechanism of gas generation during pressurized pyrolysis of a dense coal core is shown in Figure 13. The pyrolysis gas components of CH_4 and CO start to be

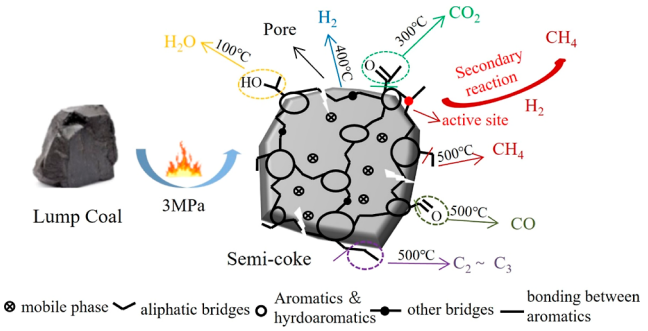

Figure 13. Pyrolysis mechanisms for gas production from coal cores.

released in large quantities at about 500 °C, while CO_2 and H_2O are generated at a lower temperature. The pressure in the pyrolysis process is a very important factor, which has an important influence on the yield and composition of the products in the pyrolysis process. According to our previous research, methane generated from the breakage of aliphatic chains in the macromolecular structure of coal coke during the pressurized pyrolysis of dense coal cores is relatively small. This was also confirmed by the online FT-IR analysis during pressurized pyrolysis. The methane in the pressurized pyrolysis comes mainly from the secondary reaction, i.e., the reaction of the active site on the coal coke with the hydrogen radical to form CH_4.[27] In summary, the rich mesoporous structure within the semicoke is not only a diffusion channel for small gas molecules but also an active site for chemical reactions between the semicoke and the gasification agent. In addition, approximately 40% of the product gas in the underground gasification of coal comes from the dry distillation drying section, where CH_4 in the product gas is mainly generated from the pyrolysis stage. Compared to shallow UCG, deep UCG is more efficient and has a better product gas composition.

https://doi.org/10.1021/acsomega.3c03327
ACS Omega 2023, 8, 40153−40161

UCG generates heat through its own combustion reaction, whereas this study provides heat through an electric heating wire, with the former generating large amounts of CO_2, hence the difference in the pyrolysis atmosphere. In addition, there is a significant temperature gradient in the dry zone of UCG, and this study has limitations in conducting tests at constant temperature conditions.

4. CONCLUSIONS

In this paper, pressurized pyrolysis experiments of coal cores were carried out through a pressurized pyrolysis device. Using FT-IR, XRD, BET, and pressurized TG−FTIR, the mechanisms of evolution of aliphatic functional groups and pore structures in semicoke during pressurized pyrolysis were revealed. The pyrolysis gas generation characteristics during pressurized pyrolysis were studied, and the conclusions are as follows:

The increase in pressure obviously changed the gas composition, most notably the relative contents of CH_4 and H_2 in the pyrolysis gas. The pressurized TG−FTIR indicated that the high external pressure hinders the release of moisture and volatiles from the primary pyrolysis process. Therefore, the gas component in the medium- and low-temperature pressurized pyrolysis process in dense coal cores is mainly controlled by secondary reactions. The intensity of the infrared absorption bands of various functional groups gradually weakened with the increase of the pyrolysis temperature, and the most significant weakening occurred at 400−500 °C, which was consistent with the generation temperature of gas components. As the pyrolysis pressure increased, the ratio of $-CH_2-/-CH_3$ became smaller, indicating that the pressure promoted the breakage of the long fat chains. With the increase of pyrolysis pressure, the surface deformation of pressurized pyrolysis semicoke increases, and the pore structure becomes more abundant. The surface deformation of the pressurized pyrolysis semicoke is more pronounced than that of the semicoke prepared under the atmosphere, with a vitreous-like substance attached to the surface and a more developed pore structure.

AUTHOR INFORMATION

Corresponding Author

Lin Xin − *College of Safety and Environmental Engineering, Shandong University of Science and Technology, Qingdao, Shandong 266590, China; Key Laboratory of Ministry of Education for Mine Disaster Prevention and Control, Shandong University of Science and Technology, Qingdao, Shandong 266590, China*; Email: xinlinsdust@sdust.edu.cn

Authors

Maofei Niu − *College of Safety and Environmental Engineering, Shandong University of Science and Technology, Qingdao, Shandong 266590, China*; orcid.org/0000-0001-6003-7671

Weimin Cheng − *College of Safety and Environmental Engineering, Shandong University of Science and Technology, Qingdao, Shandong 266590, China; Key Laboratory of Ministry of Education for Mine Disaster Prevention and Control, Shandong University of Science and Technology, Qingdao, Shandong 266590, China*

Shuqin Liu − *School of Chemical & Environmental Engineering, China University of Mining and Technology (Beijing), Beijing 100083, China*

Bowei Wang − *College of Safety and Environmental Engineering, Shandong University of Science and Technology, Qingdao, Shandong 266590, China*

Weihao Xu − *College of Safety and Environmental Engineering, Shandong University of Science and Technology, Qingdao, Shandong 266590, China*

Complete contact information is available at: https://pubs.acs.org/10.1021/acsomega.3c03327

Author Contributions

Maofei Niu: investigation, data curation, conceptualization, methodology, writing—original draft. Lin Xin: supervision, writing—review and editing. Weimin Cheng: writing—review and editing. Shuqin Liu: writing—review and editing. Bowei Wang: data curation. Weihao Xu: data curation.

Notes

The authors declare no competing financial interest.

ACKNOWLEDGMENTS

This study was financially supported by the Shandong Natural Science Foundation (no. ZR2020ME084), the National Natural Science Foundation of China (no. 51504142), the Qingchuang Science and Technology Program of Shandong Province University (no. 2019KJG008), and the SDUST Research Fund (no. 2018TDJH102).

REFERENCES

(1) Ma, W.; Li, Z.; Lv, J.; Yang, L.; Liu, S. Environmental evaluation study of toxic elements (F, Zn, Be, Ni, Ba, U) in the underground coal gasification (UCG) residuals. *J. Cleaner Prod.* **2021**, *297*, 126565.

(2) Niu, M.; Fu, Y.; Liu, S. Distribution and leachability of hazardous trace elements in Lurgi gasification ash from a Coal- to -SNG plant. *J. Energy Inst.* **2021**, *98*, 223−233.

(3) Strugala-Wilczek, A.; Kapusta, K. Migration of Co, Cd, Cu, Pb to the groundwater in the area of underground coal gasification experiment in a shallow coal seam in the experimental mine "Barbara" in Poland. *Fuel* **2022**, *317*, 122831.

(4) Yang, L.; Liang, J.; Yu, L. Clean coal technology-Study on the pilot project experiment of underground coal gasification. *Energy* **2003**, *28*, 1445−1460.

(5) Fawzy, S.; Osman, A. I.; Mehta, N.; Moran, D.; Al-Muhtaseb, A. H.; Rooney, D. W. Atmospheric carbon removal via industrial biochar systems: A techno-economic-environmental study. *J. Cleaner Prod.* **2022**, *371*, 133660.

(6) Li, W.; Zhang, S.; Lu, C. Exploration of China's net CO2 emissions evolutionary pathways by 2060 in the context of carbon neutrality. *Sci. Total Environ.* **2022**, *831*, 154909.

(7) Xin, L.; An, M.; Feng, M.; Li, K.; Cheng, W.; Liu, W.; Hu, X.; Wang, Z.; Han, L. Study on pyrolysis characteristics of lump coal in the context of underground coal gasification. *Energy* **2021**, *237*, 121626.

(8) Niu, M.; Fu, Y.; Liu, S. Mineralogical Characterization of Gasification Ash with Different Particle Sizes from Lurgi Gasifier in the Coal-to-Synthetic Natural Gas Plant. *ACS Omega* **2022**, *7*, 8526−8535.

(9) Strugała-Wilczek, A.; Stańczyk, K. Comparison of metal elution from cavern residue after underground coal gasification and from ash obtained during coal combustion. *Fuel* **2015**, *158*, 733−743.

(10) Liu, S.; Qi, C.; Jiang, Z.; Zhang, Y.; Niu, M.; Li, Y.; Dai, S.; Finkelman, R. B. Mineralogy and geochemistry of ash and slag from coal gasification in China: a review. *Int. Geol. Rev.* **2018**, *60*, 717−735.

(11) Deka, T. J.; Osman, A. I.; Baruah, D. C.; Rooney, D. W. Methanol fuel production, utilization, and techno-economy: a review. *Environ. Chem. Lett.* **2022**, *20*, 3525−3554.

(12) Khadse, A.; Qayyumi, M.; Mahajani, S.; Aghalayam, P. Underground coal gasification: A new clean coal utilization technique for India. *Energy* **2007**, *32*, 2061−2071.
(13) Wang, Z.; Liang, D.; Li, Y.; Tian, H.; Liang, J. Influence of scale and atmosphere on the pyrolysis properties of large-scale bituminous coal. *J. Anal. Appl. Pyrolysis* **2021**, *158*, 105060.
(14) Perkins, G. Underground coal gasification − Part I: Field demonstrations and process performance. *Prog. Energy Combust. Sci.* **2018**, *67*, 158−187.
(15) Xi, J.; Liang, J.; Sheng, X.; Shi, L.; Li, S. Characteristics of lump lignite pyrolysis and the influence of temperature on lignite swelling in underground coal gasification. *J. Anal. Appl. Pyrolysis* **2016**, *117*, 228−235.
(16) Liu, S.; Niu, M.; Qi, K.; Song, X.; Li, J.; He, Y.; Wang, Z.; Gao, B. Migration behavior of typical pollutants from underground coal gasification. *J. China Coal Soc.* **2018**, *43*, 2044−2051. (in Chinese)
(17) Osman, A. I.; Hefny, M.; Abdel Maksoud, M. I. A.; Elgarahy, A. M.; Rooney, D. W. Recent advances in carbon capture storage and utilisation technologies: a review. *Environ. Chem. Lett.* **2021**, *19*, 797−849.
(18) Liu, S.; Chang, Z.; Liu, J. Key technologies and prospect for in-situ gasification of deep coal resources. *J. Min. Sci. Technol.* **2021**, *6*, 261−270.
(19) Liu, H.; Guo, W.; Liu, S. Comparative techno-economic performance analysis of underground coal gasification and surface coal gasification based coal-to-hydrogen process. *Energy* **2022**, *258*, 125001.
(20) Perkins, G. Underground coal gasification − Part II: Fundamental phenomena and modeling. *Prog. Energy Combust. Sci.* **2018**, *67*, 234−274.
(21) Xin, L.; Li, K.; Feng, M.; Cheng, W.; Wang, Z.; Li, J.; Wu, J. Research on the Pollutant Migration Law Based on Large-Scale Three-Dimensional Similar Simulation Experiments of Underground Coal Gasification. *ACS Omega* **2022**, *7*, 15982−15995.
(22) Lin, D.; Liu, L.; Zhao, Y.; Zhao, Y.; Qiu, P.; Xie, X.; Sun, S. Influence of pyrolysis pressure on structure and combustion reactivity of Zhundong demineralized coal char. *J. Energy Inst.* **2020**, *93*, 1798−1808.
(23) Yu, J.; Lucas, J. A.; Wall, T. F. Formation of the structure of chars during devolatilization of pulverized coal and its thermoproperties: A review. *Prog. Energy Combust. Sci.* **2007**, *33*, 135−170.
(24) Howaniec, N. Development of porous structure of lignite chars at high pressure and temperature. *Fuel Process. Technol.* **2016**, *154*, 163−167.
(25) Zhu, Y.; Wang, Q.; Yan, J.; Cen, J.; Fang, M.; Ye, C. Influence and action mechanism of pressure on pyrolysis process of a low rank Naomaohu coal at different temperatures. *J. Anal. Appl. Pyrolysis* **2022**, *167*, 105682.
(26) Xie, X.; Liu, L.; Lin, D.; Zhao, Y.; Qiu, P. Influence of different state alkali and alkaline earth metal on chemical structure of Zhundong coal char pyrolyzed at elevated pressures. *Fuel* **2019**, *254*, 115691.
(27) Niu, M.; Wang, R.; Ma, W.; Guo, W.; Liu, H.; Liu, S. Methane formation mechanism during pressurized pyrolysis of coal core in the context of deep underground coal gasification. *Fuel* **2022**, *324*, 124668.
(28) Abdelsayed, V.; Shekhawat, D.; Smith, M. W.; Link, D.; Stiegman, A. E. Microwave-assisted pyrolysis of Mississippi coal: A comparative study with conventional pyrolysis. *Fuel* **2018**, *217*, 656−667.
(29) Ma, W.; Liu, S.; Li, Z.; Lv, J.; Yang, L. Release and transformation mechanisms of hazardous trace elements in the ash and slag during underground coal gasification. *Fuel* **2020**, *281*, 118774.
(30) Chen, Z.; Gao, S.; Xu, G. Simultaneous production of CH4-rich syngas and high-quality tar from lignite by the coupling of noncatalytic/catalytic pyrolysis and gasification in a pressurized integrated fluidized bed. *Appl. Energy* **2017**, *208*, 1527−1537.
(31) Zhang, W.; Sun, S.; Zhu, H.; Zhang, L.; Zhao, Y.; Wang, P. The evolution characteristics of bituminous coal in the process of pyrolysis at elevated pressure. *Fuel* **2021**, *302*, 120832.
(32) Chen, Y.; Zhang, L.; Zhang, Y.; Li, A. Pressurized pyrolysis of sewage sludge: Process performance and products characterization. *J. Anal. Appl. Pyrolysis* **2019**, *139*, 205−212.
(33) Chen, T.; Zhang, K.; Zheng, M.; Yang, S.; Yellezuome, D.; Zhao, R.; Liu, G.; Wu, J. Thermal properties and product distribution from pyrolysis at high heating rate of Naomaohu coal. *Fuel* **2021**, *292*, 120238.
(34) Liu, J.; Jiang, X.; Shen, J.; Zhang, H. Pyrolysis of superfine pulverized coal. Part 1. Mechanisms of methane formation. *Energy Convers. Manage.* **2014**, *87*, 1027−1038.
(35) Zhao, Y.; Qiu, P. H.; Chen, G.; Pei, J. T.; Sun, S. Z.; Liu, L.; Liu, H. P. Selective enrichment of chemical structure during first grinding of Zhundong coal and its effect on pyrolysis reactivity. *Fuel* **2017**, *189*, 46−56.
(36) Zhao, Y.; Liu, L.; Qiu, P.; Xie, X.; Chen, X.; Lin, D.; Sun, S. Impacts of chemical fractionation on Zhundong coal's chemical structure and pyrolysis reactivity. *Fuel Process. Technol.* **2017**, *155*, 144−152.
(37) Li, Q.; Wang, Z.; He, Y.; Sun, Q.; Zhang, Y.; Kumar, S.; Zhang, K.; Cen, K. Pyrolysis Characteristics and Evolution of Char Structure during Pulverized Coal Pyrolysis in Drop Tube Furnace: Influence of Temperature. *Energy Fuels* **2017**, *31*, 4799−4807.
(38) Wang, D.; Yang, H.; Wu, Y.; Zhao, C.; Ju, F.; Wang, X.; Zhang, S.; Chen, H. Evolution of pore structure and fractal characteristics of coal char during coal gasification. *J. Energy Inst.* **2020**, *93*, 1999−2005.
(39) Sadhukhan, A. K.; Gupta, P.; Saha, R. K. Characterization of porous structure of coal char from a single devolatilized coal particle: coal combustion in a fluidized bed. *Fuel Process. Technol.* **2009**, *90*, 692−700.
(40) Solomon, P. R.; Fletcher, T. H. Impact of coal pyrolysis on combustion. *Symp. (Int.) Combust.* **1994**, *25*, 463−474.
(41) Sun, S.; Xu, D.; Wei, Y.; Zhi, Y.; Jiang, G.; Guo, Y. Influence laws of operating parameters on coal pyrolysis characteristics. *J. Anal. Appl. Pyrolysis* **2022**, *167*, 105684.
(42) Howaniec, N. The effects of pressure on coal chars porous structure development. *Fuel* **2016**, *172*, 118−123.

https://doi.org/10.1021/acsomega.3c03327
ACS Omega 2023, 8, 40153−40161